Transient natural convection in a parallelogram-shaped enclosure

Jae Min Hyun and Bum Seog Choi
Department of Mechanical Engineering, Korea Advanced Institute of Science and Technology, Seoul, Korea

Transient natural convective heat transfer in a parallelogram-shaped enclosure at large Rayleigh numbers is studied. Numerical solutions to the governing Navier–Stokes equations are acquired by using a well-established finite-difference method. The possibility of utilizing this device as a transient thermal diode, by means of controlling the tilt angle of the partition walls, is investigated. Comprehensive and systematic numerical results of the evolutions of the flow and thermal fields are presented for tilt angles 0°, ±15°, ±30°, ±45°, and ±60°; and Rayleigh numbers 10^5, 10^6, and 10^7. The effects of the Prandtl number and of the aspect ratio are scrutinized. Detailed time histories of the mean Nusselt number with the tilt angle are examined. Also, numerical results of the heat transfer rates in the steady state are compiled. The steady-state results corroborate previous findings on the effectiveness of this flow configuration as a one-way heat transporting device.

Keywords: transient natural convection; parallelogram-shaped cavity; thermal diode

Introduction

Transient buoyant convection in a closed cavity at large Rayleigh numbers has received considerable attention in recent years (e.g., refs. 1 and 2). In particular, the transient process in a simple geometry, such as a rectangular enclosure with its sidewalls aligned parallel to gravity, has been widely studied. The bulk of the prior work has been concentrated on the convective process that is initiated by abruptly lowering and raising the temperatures on the two vertical sidewalls, respectively. Extensive investigations, based on scaling arguments and numerical and laboratory experimental studies, have uncovered the essential features of flow and heat transfer characteristics for the usual parameter ranges of $\mathrm{Pr} \sim 0(1)$ and $Ar \sim 0(1)$. Among others, the time scales characterizing the overall transient process, together with the global approach to steady state, have been clearly delineated.[3–6]

Studies of buoyant convection in a nonrectangular enclosure are less numerous, primarily because of analysis difficulties. However, a parallelogram-shaped cavity, as depicted in Figure 1, poses a problem of special interest. Intuitively, the flow patterns and the resulting heat transfer between the two vertical walls depend crucially on the tilt angle of the partition walls, θ. The buoyant convection, in general, is enhanced when θ is positive; conversely, the convective heat transfer is much less if θ is negative. Consequently, an important industrial application of this type of enclosure is the thermal diode wall. The practical utility of a thermal diode wall has been amply recognized in various technological applications, i.e., thermal insulation devices, solar collection panels, thermal energy storage systems, and double-glazed windows, to name a few. Several recent reports,[7–12] mostly experimental and/or numerical, have emphasized the usefulness of this relatively simple device to act as a one-way heat wall. However, the previous studies focused on the heat transfer characteristics of steady-state situations.

In the present study, we address the problem of transient buoyant convection in a parallelogram-shaped enclosure. The purpose of this study is twofold. First, in most realistic thermal systems, some forms of transient stages are involved, especially during start-up or shut-down processes. Therefore investigations of the transient convection in a parallelogram-shaped enclosure are central to the design and operation of a thermal diode. Second, apart from practical applications, the present study is significant in revealing the geometric effects of the container on the transient buoyant convection. A parallelogram-shaped cavity poses an ideal example of nonrectangular shapes that, nevertheless, possesses straightforward and explicit geometric effects.

We considered the transient buoyant adjustment process of a fluid in a two-dimensional (2-D) parallelogram-shaped enclosure when the temperatures of the two vertical sidewalls are instantaneously raised and lowered, respectively. In line with previous work,[9] the tilted walls were taken to be thermally insulating. We obtained finite-difference numerical solutions to the time-dependent Navier–Stokes equations. Complete flow and temperature data were obtained for the transient phase of buoyant convection. Nine different values of the tilt angle θ were utilized for computations. The Rayleigh numbers used range from 10^5 to 10^7; three values of the Prandtl number, $\mathrm{Pr} = 0.1$, 0.71, and 7.6, were considered; and three sets of the aspect ratio, $H/L = 0.25$, 0.5, and 1.0, were used.

The objective of the study was to describe the details of the transient flow and thermal field structures over a broad range of values for the relevant parameters. Also, as was the case for the prior work,[9] we focused on supplying complementary

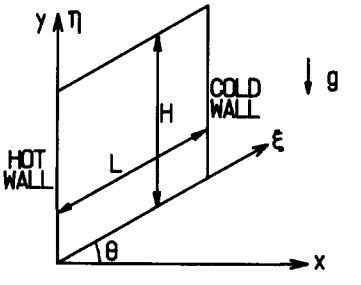

Figure 1 Flow configuration and coordinate system

Address reprint requests to Dr. Hyun at the Department of Mechanical Engineering, Korea Advanced Institute of Science and Technology, P.O. Box 150, Cheong Ryang, Seoul, Korea.

Received 17 March 1989; accepted 13 November 1989

numerical data for steady-state heat transfer characteristics, as influenced by the tilt angle and other important externally specifiable parameters.

The present numerical results for the steady state are generally consistent with the findings of preceding investigations, which employed different methods of solution. These numerical data provide useful source material against which more elaborate measurements or computations can be checked and compared.

The model

Figure 1 shows the overall flow configuration. The parallelogram-shaped cavity is filled with an incompressible viscous fluid at rest. The kinematic viscosity of the fluid is ν, the thermal diffusivity α, and the coefficient of thermometric expansion β. The fluid is in thermal equilibrium with the solid walls of the cavity at uniform temperature T_o. At $t=0$, the temperature on the left vertical sidewall is abruptly raised to T_h ($\equiv T_o+\Delta T/2$) and that of the right sidewall is lowered to T_c ($\equiv T_o-\Delta T/2$), respectively. These sidewall temperatures are maintained at the same levels thereafter. The tilted walls are assumed to be thermally insulating. The size of the cavity is characterized by the height H and the tilted wall length L. Consideration is confined to 2-D flow fields, and the ensuing fluid motion and attendant heat transfer are to be described.

As Figure 1 shows, the relationships between the cartesian coordinates (x, y) and the cavity surface coordinates (ξ, η) are

$$x=L\xi\cos\theta \quad \text{and} \quad y=L\eta+L\xi\sin\theta \tag{1}$$

The governing equations are the time-dependent Navier–Stokes equations, with the Boussinesq fluid assumption incorporated. Expressed in the vorticity(ζ)–stream function(Ψ) formulation, these equations, written in nondimensional form, are well known (e.g., refs. 7–10):

$$\frac{\partial\zeta}{\partial\tau}+\frac{1}{\cos\theta}\left[U\frac{\partial\zeta}{\partial\xi}+V\frac{\partial\zeta}{\partial\eta}\right]=\frac{\mathrm{Pr}}{\cos^2\theta}\left[\frac{\partial^2\zeta}{\partial\xi^2}-2\sin\theta\frac{\partial^2\zeta}{\partial\xi\,\partial\eta}+\frac{\partial^2\zeta}{\partial\eta^2}\right]+\frac{\mathrm{Pr\,Ra}}{\cos\theta}\left[\frac{\partial T^*}{\partial\xi}-\sin\theta\frac{\partial T^*}{\partial\eta}\right] \tag{2}$$

$$\frac{\partial T^*}{\partial\tau}+\frac{1}{\cos\theta}\left[U\frac{\partial T^*}{\partial\xi}+V\frac{\partial T^*}{\partial\eta}\right]=\frac{1}{\cos^2\theta}\times\left[\frac{\partial^2T^*}{\partial\xi^2}+2\sin\theta\frac{\partial^2T^*}{\partial\xi\,\partial\eta}+\frac{\partial^2T^*}{\partial\eta^2}\right] \tag{3}$$

$$\frac{1}{\cos^2\theta}\left[\frac{\partial^2\Psi}{\partial\xi^2}-2\sin\theta\frac{\partial^2\Psi}{\partial\xi\,\partial\eta}+\frac{\partial^2\Psi}{\partial\eta^2}\right]=-\zeta \tag{4}$$

where U and V denote, respectively, the velocity components in the (ξ, η) direction; i.e.,

$$U=\frac{\partial\Psi}{\partial\eta} \quad \text{and} \quad V=-\frac{\partial\Psi}{\partial\xi} \tag{5}$$

In Equations 2–5, the nondimensional quantities are defined as

$$\tau=\frac{\alpha t}{L^2} \qquad T^*=\frac{T-T_o}{T_h-T_c} \qquad \Psi=\frac{\psi}{\alpha} \qquad \zeta=\frac{L^2\omega}{\alpha}$$

$$Ar=\frac{H}{L} \qquad \mathrm{Pr}=\frac{\nu}{\alpha} \quad \text{and} \quad \mathrm{Ra}=\frac{g\beta L^3(T_h-T_c)}{\nu\alpha}$$

The appropriate boundary conditions are

$U=V=0$ on all solid boundaries

$T^*=0.5$ on $\xi=0$

$T^*=-0.5$ on $\xi=1$

$\dfrac{\partial T^*}{\partial n}=0$ on $\eta=0, 1$

where n denotes the direction normal to the tilt walls.

The numerical techniques for solving Equations 2–4 have been well established by many previous investigators. We chose a modified version of the finite-difference method originally developed by Küblbeck *et al.*[13] The algorithm based on this methodology has been successfully applied to a number of transient buoyant convective flows in an enclosure.[14,15] Sensitivity tests of grid size for this particular algorithm were previously carried out in detail (see Figure 6 of ref. 13 and Figure 2 of ref. 15). Similar tests for the present numerical solutions were conducted for several runs, and the results were quite satisfactory. In the present computations, the mesh points employed were typically (33 × 33) for the case of $Ar=1.0$. The grid points were appropriately increased to handle the cases of higher Rayleigh numbers.

Results and discussion

Transient evolutions of flow and temperature fields are depicted in Figure 2 for $\mathrm{Ra}=10^7$, $\mathrm{Pr}=7.6$, and $Ar=1.0$. The qualitative

Notation

Ar	Aspect ratio, H/L
H	Height of the enclosure
L	Length of the tilted wall
Nu_m	Mean Nusselt number
Pr	Prandtl number, ν/α
Ra	Rayleigh number, $g\beta L^3\,\Delta T/\nu\alpha$
t	Dimensional time
T, T^*	Dimensional and nondimensional temperature
ΔT	Wall temperature difference, T_h-T_c
U, V	Nondimensional velocity components
x, y	Cartesian coordinates

Greek symbols

ξ, η	Nondimensional transformed coordinates: $\xi=\dfrac{x}{L\cos\theta}$; $\eta=\dfrac{y-x\tan\theta}{L}$
α	Thermal diffusivity
β	Coefficient of volumetric expansion
θ	Tilt angle
τ, τ^*	Nondimensional and scaled nondimensional time: $\tau=\dfrac{\alpha t}{L^2}$; $\tau^*=\tau\left(\dfrac{\mathrm{Ra}}{Ar}\right)^{1/4}$
ν	Kinematic viscosity
ψ, Ψ	Dimensional and nondimensional stream function
ω, ζ	Dimensional and nondimensional vorticity

Subscripts

o	Reference value
h	Hot wall
c	Cold wall
m	Mean value

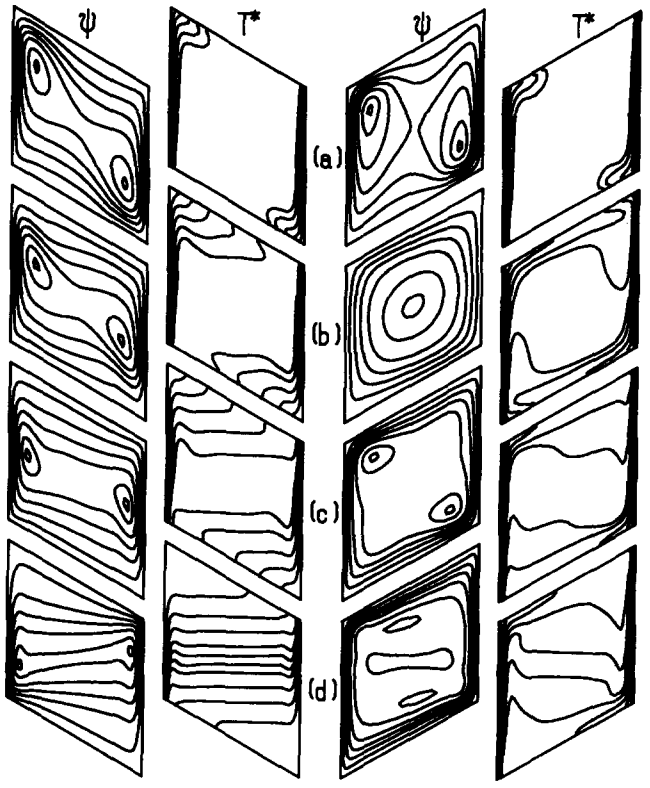

Figure 2 Plots of streamfunction Ψ and isotherms T^*. $Ra=10^7$, $Pr=7.6$, and $Ar=1.0$. The left two columns are for $\theta=-30°$, and the right two columns are for $\theta=30°$. The scaled nondimensional times, $\tau^*[\equiv(Ra/Ar)^{1/4}\tau]$, are (a) $\tau^*=0.04$; (b) $\tau^*=0.1$; (c) $\tau^*=0.2$; (d) $\tau^*=2.0$

changes, depending on whether θ takes a positive or negative value, are noticeable in both the flow and thermal structures. The general results for a positive θ, i.e., a thermally destabilizing case, are illustrated in the right two columns of Figure 2. At early times, the boundary layers are formed by conductive heat transfer from the vertical sidewalls, which produces two cells in the flow fields. At intermediate times, two cells move into the interior core region and merge into a single cell as buoyant convective activities become vigorous. Because of these strong convective motions, overshooting appears in the thermal field at moderate times. As more time elapses, overshooting tends to subside and the amplitudes of fluid motions are reduced. In the bulk of the interior, as the steady state is approached, the thermal field is fairly linearly stratified in the vertical direction; however, the horizontal temperature gradients are not insignificant. Here, for computational purposes, we assert that the steady state has been achieved if the temporal variations of all flow variables are less than 0.1% over a time interval of $0.1\tau^*$, where τ^* is the nondimensional heat-up time scale, defined as $\tau^*=\tau(Ra/Ar)^{1/4}$.[3-6] This condition is usually attained within $2\tau^*$. We further discuss the approach to steady state later in connection with the behavior of the mean Nusselt numbers on the vertical walls. The global flow characteristics described are representative of the solutions when the tilt angle θ is positive, although some minor quantitative differences may occur, depending on the precise values of the other prevailing physical parameters.

When the tilt angle θ is negative, i.e., the thermally stabilizing vertical wall conditions, the results are demonstrated in the left two columns of Figure 2. The early time behavior of the conduction-dominant stage is similar to that of the case of a positive θ. However, at moderate times, owing to the stabilizing effect of buoyancy, the convective activities are less vigorous than for a positive θ. The two cells do not merge into a single cell in the interior, and no appreciable overshooting appears in the thermal field. As time elapses, the flow lessens, and in much of the interior region the temperature field exhibits nearly complete linear stratification in the vertical direction.

The principal differences in the character of flow, depending on the sign of the tilt angle θ, are more pronounced for a larger θ, as clearly shown in Figure 3 for $\theta=\pm60°$. For $\theta=60°$, intensification of convective activities at moderate times, together with overshooting in the thermal field, is more drastic than for $\theta=30°$. Consequently, even at the steady-state limit, the thermal structure in the bulk of the interior region has substantial horizontal gradients superposed on the dominant vertical gradients. Because of these large horizontal temperature gradients, vertical stratification in the interior region deviates considerably from a strictly linear profile. On the other hand, for $\theta=-60°$, the convective flows at moderate times are less vigorous than for $\theta=60°$; consequently, no single-cell structure emerges. Also, the isotherms do not exhibit noticeable overshooting. The temperature field in the interior undergoes a relatively smooth stratifying process; no eminent horizontal temperature gradients are discernible in much of the interior region at intermediate stages. At extended times leading to the steady state, temperature stratification shows a nearly perfect vertical linear profile in the majority of the central portions of the interior core. Interestingly, localized regions of substantial

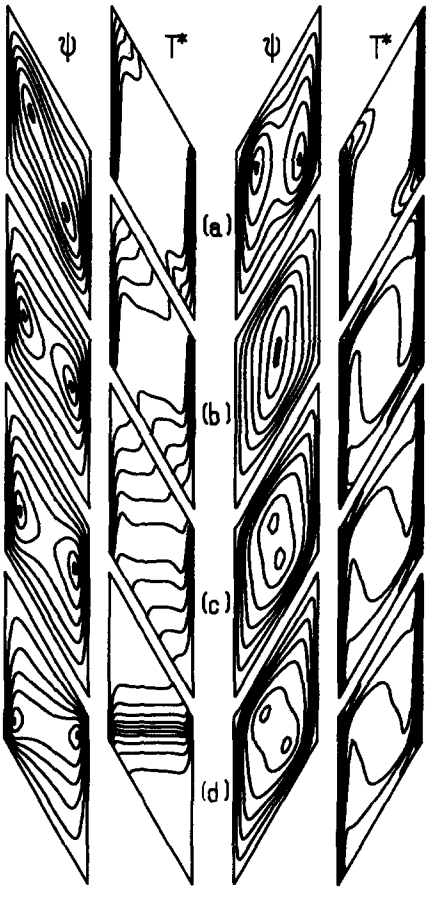

Figure 3 Plots of streamfunction Ψ and isotherms T^*. $Ra=10^7$, $Pr=7.6$, and $Ar=1.0$. The left two columns are for $\theta=-60°$, and the right two columns are for $\theta=60°$. The scaled nondimensional times, $\tau^*[\equiv(Ra/Ar)^{1/4}\tau]$, are (a) $\tau^*=0.04$; (b) $\tau^*=0.1$; (c) $\tau^*=0.2$; (d) $\tau^*=2.0$

Figure 4 Plots of streamfunction Ψ and isotherms T^*. $Ra=10^6$, $Pr=7.6$, and $Ar=0.25$. The left two columns are for $\theta=-60°$, and the right two columns are for $\theta=60°$. The scaled nondimensional times, $\tau^*[\equiv (Ra/Ar)^{1/4}\tau]$, are (a) $\tau^*=0.04$; (b) $\tau^*=0.1$; (c) $\tau^*=0.2$; (d) $\tau^*=2.0$

size exist in the upper left and lower right corners, within which the temperatures are almost uniform.

The computed results illustrated by Figures 2 and 3 clearly demonstrate the major differences in flow properties between the cases of positive θ and negative θ. These flow and temperature fields qualitatively represent all the results computed for the parameter ranges considered in the present study for $Ar\sim 0(1)$, although details do reveal minor differences depending on the specific parameter variations.

Figure 4 displays the results for a small aspect ratio, $Ar=0.25$. For positive θ, the flow is driven by conduction at early times. However, since the length of the tilted partition walls is substantial, at intermediate times and afterward the thermal field contains two rather well-defined regions: conduction-dominant areas close to the vertical sidewalls; and the interior core, in which the influence of convection is prominent. At the steady-state limit, the bulk of the flow field is filled with a convection cell of appreciable magnitude; the isotherms in the interior are aligned parallel to the plane of the partition walls. For negative θ, the early time behavior is conduction controlled. However, at moderate and extended times, the isotherms move away from the vertical sidewalls, aided by the relatively weak convective activities. The steady-state stage is characterized by the interior region in which nearly linear vertical stratification is attained. In small localized areas close to the left upper and right lower corners, the fluid motions are suppressed, and the temperatures in these regions are nearly uniform.

In an effort to understand flow evolution within the vertical boundary layer, we plotted in Figure 5 the time histories of the vertical velocity at a point adjacent to the hot left wall. The velocity initially increases rapidly to a peak value and then decreases relatively slowly to approach its steady-state value. The overall adjustment time is $\tau^*\sim 0(1)$, where $\tau^*=(Ra/Ar)^{1/4}(\alpha/L^2)t$. This result generally agrees qualitatively with previous findings on transient convection in an enclosure.[3–6] Also, the temporal variations of the mean heat transfer rates are very small after about $2\tau^*$. This condition reinforces our earlier assertion that the numerical data contained in Figures 2–4 are representative of steady-state features.

Figures 6 and 7 illustrate the time histories of the mean Nusselt number Nu_m on the hot vertical sidewall. The time to accomplish the global adjustment to the steady state is given by $\tau^*\sim 0(1)$. This result suggests that the overall heat-up time scale, originally derived for a rectangular geometry,[1–6] by and large, also applies to a parallelogram-shaped container. The heat-up time scale measures the global time for buoyant convection-driven flows to attain the overall adjustment inside much of a cavity. As Figures 6 and 7 indicate, the dominant time scales for global adjustment are rather insensitive to variations in the tilt angle θ.

The time-history patterns represented by Figure 6 reveal qualitative features similar to the solutions acquired for high-Rayleigh number, transient-convective processes in a square cavity (e.g., see refs. 1, 14). However, details of the temporal behavior of Nu_m, as revealed in Figures 6 and 7, appear to be influenced heavily by the geometric particulars of the cavity.

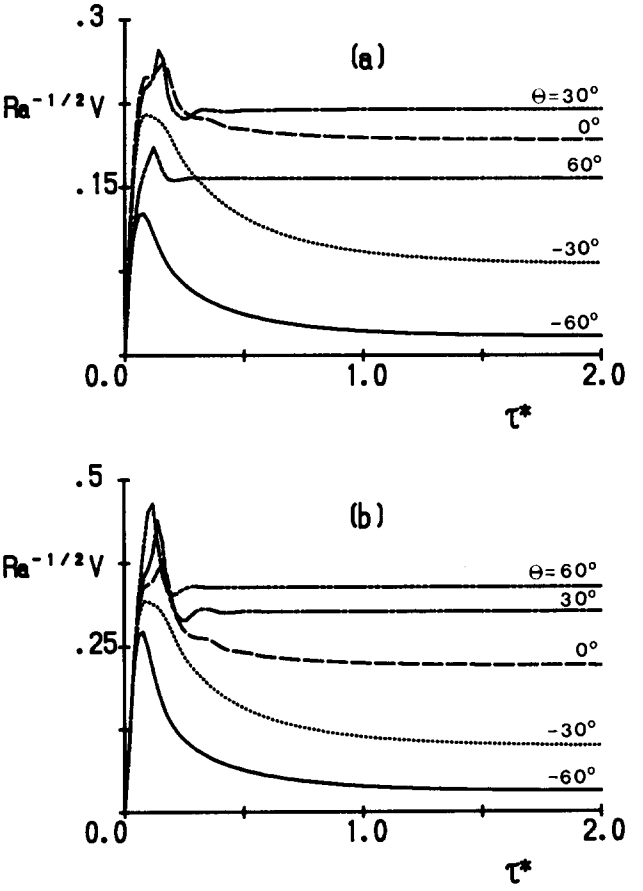

Figure 5 Representative plots of the vertical velocity V near the vertical wall versus time. $Ra=10^6$, $Pr=7.6$, and $Ar=1.0$. The positions are (a) $\xi=0.012$, $\eta=0.5$; (b) $\xi=0.057$, $\eta=0.5$

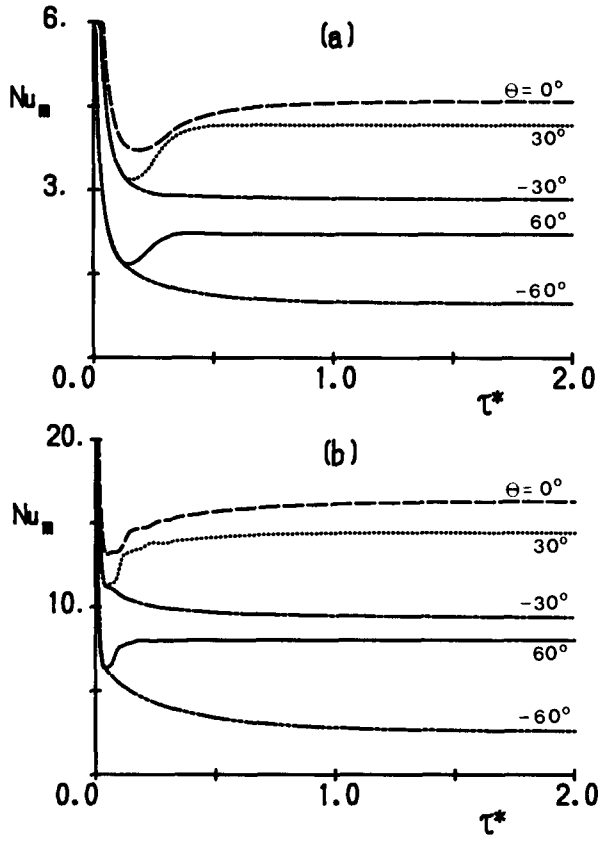

Figure 6 Mean Nusselt number Nu_m versus the scaled time τ^*. Pr=7.6 and Ar=1.0. (a) Ra=10^5; (b) Ra=10^7

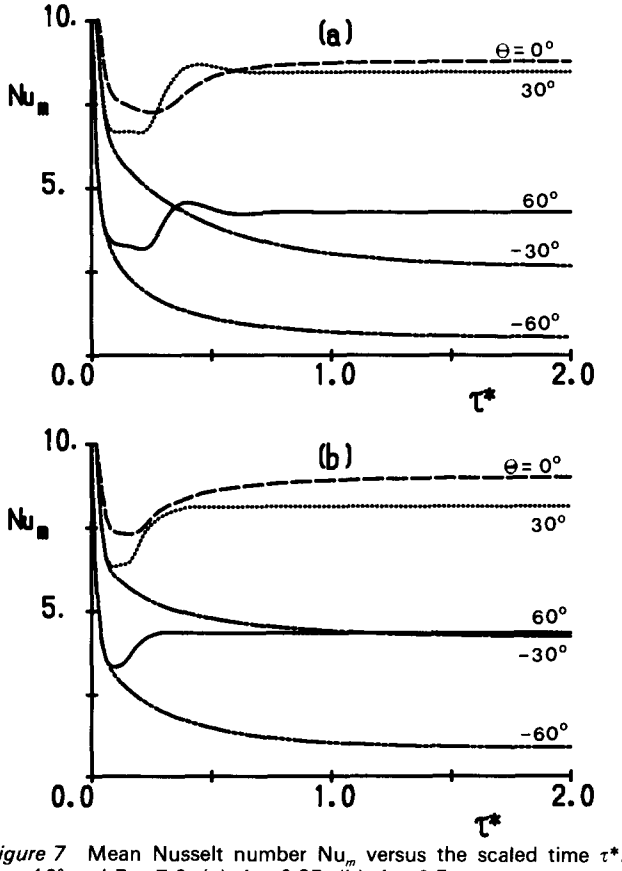

Figure 7 Mean Nusselt number Nu_m versus the scaled time τ^*. Ra=10^6 and Pr=7.6. (a) Ar=0.25; (b) Ar=0.5

One consideration is that the effective area of the cavity varies with the tilt angle; another is that the intensity of the convective motions depends strongly on the tilt angle, as has been amply documented. Therefore, for a large positive tilt angle, both the reduction of the cavity area and the intensification of the convective activities enable the flow to reach the steady state within a relatively short time span. As Figure 7 also indicates for a smaller aspect ratio, the length of the insulating partition walls, over which the convectively driven fluid has to travel, increases; consequently, the time of adjustment tends to increase as the aspect ratio decreases.

It is also noteworthy that in the steady state, as the aspect ratio decreases, the ratio of the maximum Nu_m at positive θ to the minimum Nu_m at negative θ increases. For instance, this ratio is nearly 8.0 when $\theta = \pm 60°$ at Ra=10^6, Pr=7.6, and Ar=0.25, whereas this ratio is only 2.8 when Ar=1.0 with the other parameters being the same. This finding is significant in that the aspect ratio strongly influences the effectiveness of a one-way heat transfer device.

Upon compiling the comprehensive numerical data, we systematically analyzed the steady-state heat transfer rate to gain further insight into the effects of the various parameters. Previous studies, both experimental and numerical, have already provided a growing body of information concerning the steady-state values of Nu_m. In this regard, the present study supplements and reinforces the existing data. Figure 8 compares the present numerical data with prior results.[9,10] The present numerical results for Ra=10^5 closely agree with the previous

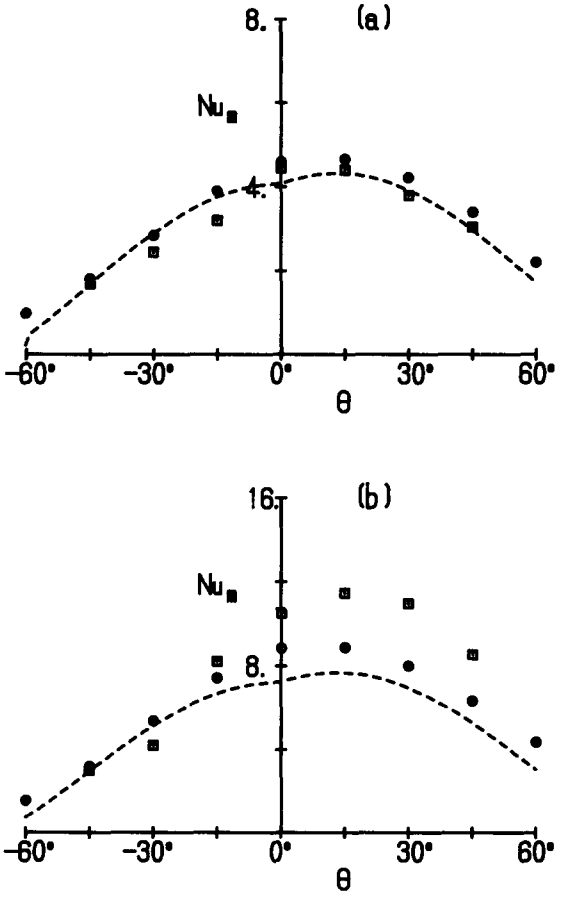

Figure 8 Variation of the steady-state mean Nusselt number Nu_m with tilt angle θ. Ar=1.0. (a) Ra=10^5; (b) Ra=10^6. ○: present numerical solution; □: experimental result from ref. 9; ----: empirical formula from ref. 10

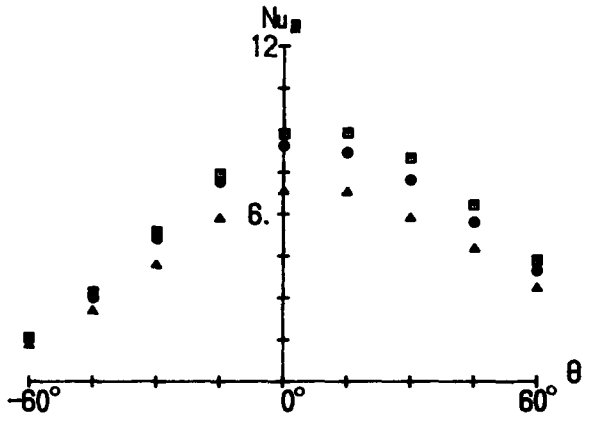

Figure 9 Variation of the steady-state mean Nusselt number Nu_m with tilt angle θ. $Ar=1.0$ and $Ra=10^6$. △: $Pr=0.1$; ○: $Pr=0.71$; □: $Pr=7.6$

experimental data. For the case of $Ra=10^6$, agreement is somewhat less when θ is positive. However, overall consistency among the various results is apparent.

Finally, we focused on the effect of Prandtl number on the mean heat transfer rate in the steady state. Figure 9 summarizes the numerical results of the steady-state mean Nusselt number Nu_m obtained by using $Ra=10^6$ and three different Prandtl numbers, $Pr=0.1$, 0.71, and 7.6. The qualitative trend of Nu_m with varying tilt angles is largely unaffected by the change in Pr. However, Nu_m generally increases slightly as Pr increases. This observation is in accord with previous findings for the case of a rectangular cavity.[15,16]

Conclusions

Extensive numerical calculations were carried out to assess the transient natural convection in a parallelogram-shaped enclosure when the vertical sidewalls are instantaneously heated differentially. Depending on whether θ is positive or negative, evolution of the flow and thermal structures vary markedly. For negative θ, the temperature field in the interior undergoes a relatively smooth stratifying process, and the temperature gradients in the interior are largely vertical at the intermediate stages. For positive θ, appreciable horizontal temperature gradients are superimposed on the dominant vertical gradients.

Small values of the aspect ratio appear to play a significant role in enhancing the effectiveness of a one-way thermal diode. A large amount of transient flow and thermal field data has been analyzed to produce time histories of the behavior of Nu_m.

The steady-state data of the present numerical computations agree satisfactorily with the previously reported results. The steady-state results of the present calculations supplement evidence used to ascertain the effectiveness of the diode as a one-way heat wall.

Acknowledgment

This work was supported, in part, by a research grant from the Korea Science and Engineering Foundation.

References

1 Patterson, J. and Imberger, J. Unsteady natural convection in a rectangular cavity. *J. Fluid Mech.*, 1980, **100**, 65–86

2 Ivey, G. N. Experiments on transient natural convection in a cavity. *J. Fluid Mech.*, 1984, **144**, 389–401

3 Hyun, J. M. Transient buoyant convection of a contained fluid driven by the changes in the boundary temperatures. *ASME J. Appl. Mech.*, 1985, **52**, 193–198

4 Hyun, J. M. Transient process of thermally stratifying an initially homogeneous fluid in an enclosure. *Int. J. Heat Mass Transfer*, 1984, **27**, 1936–1983

5 Sakurai, T. and Matsuda, T. A temperature adjustment process in a Boussinesq fluid via a buoyancy induced meridional circulation. *J. Fluid Mech.*, 1972, **54**, 417–421

6 Jischke, M. C. and Doty, R. T. Linearized buoyant motion in a closed container. *J. Fluid Mech.*, 1975, **71**, 729–754

7 Nakamura, H. and Asako, Y. Heat transfer in a parallelogram-shaped enclosure. *Bull. JSME*, 1980, **23**, 1827–1834

8 Nakamura, H. and Asako, Y. Heat transfer in a parallelogram-shaped enclosure. *Bull. JSME*, 1982, **25**, 1412–1418

9 Maekawa, T. and Tanasawa, I. Natural convection heat transfer in parallelogrammic enclosures. *Proc. 7th Int. Heat Transfer Conf.*, München, vol. 2. Hemisphere, Washington, D.C., 1982, 227–232

10 Seki, N., Fukusako, S., and Yamaguchi, A. An experimental study of free convective heat transfer in a parallelogrammic enclosure. *ASME J. Heat Transfer*, 1983, **105**, 433–439

11 Chung, K. C. and Trefethen, L. M. Natural convection in a vertical stack of inclined parallelogrammic cavities. *Int. J. Heat Mass Transfer*, 1982, **25**, 277–284

12 Ashjaee, M., Mitchell, J. W., and El-Wakil, M. M. Natural convection in vertical enclosures partitioned at different angles. *ASME HTD*, 1986, **63**, 1–7

13 Küblbeck, K., Merker, G. P., and Straub, J. Advanced numerical computation of two-dimensional time-dependent free convection in cavities. *Int. J. Heat Mass Transfer*, 1980, **23**, 203–217

14 Hyun, J. M. and Lee, J. W. Transient natural convection in a square cavity of a fluid with temperature-dependent viscosity. *Int. J. Heat and Fluid Flow*, 1988, **9**, 278–285

15 Hyun, J. M. and Lee, J. W. Numerical solutions for transient buoyant convection in a square cavity with different sidewall temperatures. *Int. J. Heat and Fluid Flow*, 1989, **10**, 146–151

16 Mallinson, G. D. and Davis G. De Vahl. Three-dimensional natural convection in a box: A numerical study. *J. Fluid Mech.*, 1977, **83**, 1–31